

Energy of the Quasi-free Electron in Dense Neon

C. M. Evans^{a,b,*} Yevgeniy Lushtak^{a,b} G. L. Findley^c

^a*Department of Chemistry and Biochemistry, Queens College – CUNY, Flushing,
NY 11367*

^b*Department of Chemistry, Graduate Center – CUNY, New York, NY 10016*

^c*Department of Chemistry, University of Louisiana at Monroe, Monroe, LA
71209, United States*

Abstract

In this Letter, field ionization of O₂ doped into Ne is used to extract the minimum energy V_0 of the conduction band in dense Ne, and a novel critical point effect is observed. These results represent the first complete view of V_0 from low density to the density of the triple point liquid for a repulsive fluid (i.e., a fluid with a positive zero-kinetic-energy electron scattering length). The recently developed local Wigner-Seitz model is shown to fit these data accurately both at noncritical temperatures and on an isotherm near the critical isotherm.

Key words: Wigner-Seitz model, dense neon, field ionization, quasi-free electron energy, critical point effects

PACS: 33.15.Ry, 34.30.+h, 31.70.-f, 31.70.Dk

* Corresponding author.

Email addresses: cherice.evans@qc.cuny.edu (C. M. Evans),

1 Introduction

Critical point effects on the energy and lineshape of absorption, fluorescence, and vibrational bands of dopants as a function of a perturber fluid number density ρ_P have been observed by various groups [1,2]. We have recently begun to investigate how density fluctuations in near critical point fluids affect the energy of the quasi-free electron [3–8]. Studies of the minimum energy $V_0(\rho_P)$ of the conduction band in the attractive fluids Ar [3, 4, 7, 9, 10], Kr [5, 7, 9, 10], Xe [6,7], CH₄ [8] and C₂H₆ [8] (with an attractive fluid being one that possesses a negative zero-kinetic-energy electron scattering length) showed a dramatic change (i.e., a 0.1 – 0.3 eV increase) in $V_0(\rho_P)$ near the critical point. This observation led to the development of a local Wigner-Seitz model for $V_0(\rho_P)$ that represents an order of magnitude improvement over previous theoretical treatments [3–10].

Detailed studies of $V_0(\rho_P)$ in repulsive fluids (i.e., fluids with a positive zero-kinetic-energy electron scattering length), however, have been stymied by the very low critical temperatures and triple point temperatures exhibited by these fluids. In this Letter, we report field ionization of O₂ doped into Ne, and then use these data to extract $V_0(\rho_{Ne})$. This study represents the first detailed investigation of $V_0(\rho_P)$ in a repulsive fluid from low density to the density of the triple point liquid, both at noncritical temperatures and on an isotherm near the critical isotherm. We are thereby able to show that the local Wigner-Seitz model can be extended to repulsive systems.

findley@ulm.edu (G. L. Findley).

2 Experimental

As in our earlier work [3–10], photoionization spectra of O₂ in Ne were measured with monochromatic synchrotron radiation having a resolution of 10 meV in the spectral region of interest. The copper sample cell is equipped with entrance and exit LiF windows and a pair of parallel plate electrodes (stainless steel, 3.0 mm spacing) oriented parallel to the incoming radiation and perpendicular to the windows. The temperature of the cell was maintained to ± 0.5 K at noncritical temperatures and to ± 0.3 K near the critical temperature of Ne (i.e., $T_r = T/T_c = 1.02$, where $T_c = 44.4$ K) using an open flow liquid helium cryostat and resistive heater attached to the sample cell. In order to shift the energy cut-off of the LiF window to above the ionization energy of O₂, all data were obtained at temperatures below 73 K. O₂ (Matheson Gas Products, 99.998%) and Ne (AirGas, 99.999%) were used without further purification, and the lack of impurity interference was verified by both transmission and photoionization spectroscopy. Prior to the introduction of a sample, the gas handling system (GHS) was baked to a base pressure of low 10^{-8} Torr; after adding O₂, the GHS was allowed to return to the low 10^{-7} Torr range prior to the introduction of Ne. The O₂ concentration was maintained at < 10 ppm.

3 Results and Discussion

We used field ionization of high- n O₂ Rydberg states in order to determine the O₂ ionization threshold with minimal scatter across the wide temperature and density range of this study. In this method [8, 11], the difference is taken

between two photoionization spectra measured with different applied electric fields (after intensity normalizing the spectra to remove the effects of secondary ionization), which yields a peak that represents those Rydberg states ionized by the high electric field F_H but not by the low field F_L . Both F_L and F_H were optimized to produce the best field ionization signal for each Ne density, with $F_L = 4,600 - 8,300$ V/cm and $F_H = 8,300 - 13,000$ V/cm. (Since the time scale required for electron localization [12] in these high electric fields is significantly longer than that for the dopant photoionization process, electron localization in Ne does not occur during these measurements. O_2 can form a stable negative ion in some solvents [13] with a rate constant that depends both on the solvent density and on the electric field strength. At the electric field strengths chosen for this experiment, we observed no changes in the field ionization spectra indicative of negative ion formation.) The energy shift ΔI of the field ionization peak is given by [8,9]

$$\Delta I = -c_0 (F_L^{1/2} + F_H^{1/2}), \quad (1)$$

where $c_0 = 4.2 \pm 0.7 \times 10^{-4}$ eV cm^{1/2} V^{-1/2} is the field ionization constant for O_2 . (The field ionization constant c_0 and the gas phase O_2 ionization energy $I_g = 12.065 \pm 0.005$ eV were empirically determined from field ionization studies of neat O_2 at various electric field strengths.) The Ne induced shift $\Delta(\rho_{Ne})$ in the O_2 ionization energy, after correcting for the electric fields, is [8,9]

$$\Delta(\rho_{Ne}) = I_F(\rho_{Ne}) + c_0 (F_L^{1/2} + F_H^{1/2}) - I_g, \quad (2)$$

where $I_F(\rho_{Ne})$ is the energy of the maximum of the O_2 field ionization peak at the Ne density ρ_{Ne} . Fig. 1 shows $\Delta(\rho_{Ne})$ plotted as a function of reduced Ne number density $\rho_r \equiv \rho_{Ne}/\rho_c$, where the critical density of Ne is $\rho_c = 14.4 \times 10^{21}$ cm⁻³ [14]. The total error for these measurements is given by a sum of the

field correction error, the goodness-of-fit error (for fitting a field ionization spectrum to a Gaussian line shape), and the error arising from the energy uncertainty due to the resolution of the monochromator (i.e., ± 5 meV). This total experimental error is between 15 and 25 meV for the entire density range.

Although field ionization allows one to determine the perturber induced shift $\Delta(\rho_{\text{Ne}})$ accurately at all Ne number densities, this shift does not represent the minimum energy $V_0(\rho_{\text{Ne}})$ of the conduction band of Ne. The relationship between $\Delta(\rho_{\text{Ne}})$ and $V_0(\rho_{\text{Ne}})$ is [8, 9]

$$V_0(\rho_{\text{Ne}}) = \Delta(\rho_{\text{Ne}}) - P_+(\rho_{\text{Ne}}), \quad (3)$$

where $P_+(\rho_{\text{Ne}})$ is the ensemble-averaged O_2^+/Ne polarization energy. $P_+(\rho_{\text{Ne}})$ was calculated from [8, 9, 15]

$$P_+(\rho_{\text{Ne}}) = -4\pi\rho_{\text{Ne}} \int_0^\infty g_{\text{DP}}(r) w_+(r) r^2 dr, \quad (4)$$

where $g_{\text{DP}}(r)$ is the O_2/Ne radial distribution function and $w_+(r)$ is the O_2^+/Ne interaction potential. The dopant/perturber O_2/Ne radial distribution function $g_{\text{DP}}(r)$ and the Ne/Ne radial distribution function $g(r)$ were calculated using the coupled Percus-Yevick equations [8, 16] for dilute binary systems using Lennard-Jones 6-12 potentials for both the Ne/Ne and O_2/Ne interactions. (The Ne/Ne potential parameters [17] were $\sigma = 2.782 \text{ \AA}$ and $\varepsilon/k_B = 37.3 \text{ K}$, where $k_B \equiv$ Boltzmann's constant. The O_2/Ne potential parameters were determined from the Sikora combining rules [18], although small (i.e., $< 1\%$) adjustments were made in the parameters to obtain the best fit to experiment. The final O_2/Ne Lennard-Jones 6-12 potential parameters were $\sigma = 3.128 \text{ \AA}$ and $\varepsilon/k_B = 50.5 \text{ K}$.) $P_+(\rho_{\text{Ne}})$ determined from eq. (4) is plotted as a function of reduced Ne number density ρ_r in Fig. 2, with the strong critical point effect

being due to an increase in Ne clustering around O₂ near the critical density and temperature of Ne.

Fig. 3 presents $V_0(\rho_{\text{Ne}})$ as extracted from the data of Fig. 1 using eq. (3) and the $P_+(\rho_{\text{Ne}})$ of Fig. 2. Unlike the previous results for the attractive gases [3–10], it is obvious that $V_0(\rho_{\text{Ne}})$ is strictly positive. Thus, Ne represents a prototypical repulsive fluid and, therefore, can be used to test the applicability of the local Wigner-Seitz model to these fluids. In this model, for any given perturber, $V_0(\rho_{\text{P}})$ is specified by [8, 9]

$$V_0(\rho_{\text{P}}) = P_-(\rho_{\text{P}}) + E_k(\rho_{\text{P}}) + \frac{3}{2} k_B T, \quad (5)$$

where $P_-(\rho_{\text{P}})$ is the ensemble-averaged electron/perturber polarization energy, $E_k(\rho_{\text{P}})$ is the zero-point kinetic energy of the quasi-free electron, and $(3/2) k_B T$ is the thermal energy of the quasi-free electron. $P_-(\rho_{\text{P}})$ is determined from [8, 9, 15]

$$P_-(\rho_{\text{P}}) = -4\pi\rho_{\text{P}} \int_0^\infty g(r) w_-(r) r^2 dr, \quad (6)$$

where $g(r)$ is the perturber/perturber radial distribution function, and $w_-(r)$ is the electron/perturber interaction potential. Any critical point behavior in $P_-(\rho_{\text{P}})$ arises from variations in $g(r)$ near the critical density and temperature.

The zero-point kinetic energy $E_k(\rho_{\text{P}})$ is obtained from solving the Schrödinger equation

$$\nabla^2\psi + \frac{2m_e}{\hbar^2} [E_k - V_{loc}(r)]\psi = 0 \quad (7)$$

for the quasi-free electron in a dense perturber. In eq. (7), $V_{loc}(r)$ is a short-ranged potential that accounts for local dynamic polarization of a perturber by the optical electron, m_e is the mass of the electron, and \hbar is the reduced Planck constant. The local potential $V_{loc}(r)$ satisfies an average translational

symmetry $V_{loc}(r) = V_{loc}(r + 2r_b)$, where r_b is the interaction range. At any density, the minimum distance between a quasi-free electron with low kinetic energy and a single perturber is given by the absolute value of the scattering length A . At high perturber number densities, under the assumption that interactions in the first solvent shell dominate the dynamics of the problem, the maximum distance r_ℓ for a short-ranged interaction is one-half of the spacing between two perturber atoms in the first solvent shell. This maximum spacing, otherwise known as the local Wigner-Seitz radius [8, 9], is

$$r_\ell = \sqrt[3]{\frac{3}{4\pi g_m \rho_P}} \quad (8)$$

where g_m is the maximum of $g(r)$. Thus, the interaction range for the local short-ranged potential is $r_b = r_\ell - |A|$. By applying these conditions to the asymptotic solutions of eq. (7), the zero-point kinetic energy of the quasi-free electron is [8, 9]

$$E_k(\rho_P) = \frac{\hbar^2 \eta_0^2}{2m_e (r_\ell - |A|)^2} \cdot \quad (9)$$

In eq. (9), η_0 is the phase shift induced by the short-ranged potential, and the density dependence arises from r_ℓ . Thus, any critical point behavior in $E_k(\rho_P)$ will result from a change in r_ℓ near the critical density along the critical isotherm due to density fluctuations that are reflected in g_m . The phase shift η_0 is empirically determined to give the best fit to experiment.

The lines in Fig. 3 are the results of local Wigner-Seitz calculations using eq. (5), with the $P_-(\rho_{Ne})$ and $E_k(\rho_{Ne})$ functions given in Figs. 4 and 5, respectively. The radial distribution function $g(r)$ for Ne was determined simultaneously with $g_{DP}(r)$ for O₂/Ne. The scattering length and the phase shift necessary for determining $E_k(\rho_{Ne})$ were $A = 0.10 \text{ \AA}$ [20] and $\eta_0 = 0.65$, respectively. ($V_0(\rho_P)$ was also modeled at selected densities using a Morse potential [21] for

the Ne/Ne interactions. This led to no appreciable improvement in the quality of the fit to the experimental data.)

Clearly, the local Wigner-Seitz model works equally well for the repulsive gas Ne as it does for the attractive gases [3–9], and predicts the extracted $V_0(\rho_{\text{Ne}})$ both for the noncritical temperatures and on an isotherm near the critical isotherm. The strictly positive nature of $V_0(\rho_{\text{Ne}})$ can be explained from a closer inspection of Figs. 4 and 5.

In the local Wigner-Seitz model, the electron/perturber interaction is dominated by the perturber/perturber interactions, which are governed by the choice of intermolecular potential. Fig. 4 shows that the polarization energy $P_-(\rho_{\text{Ne}})$ at the density of the triple point liquid is ~ -0.5 eV, which is significantly smaller than that for the attractive rare gases (i.e., ~ -1.0 to -1.6 eV [3–7]). The zero-point kinetic energy $E_k(\rho_{\text{Ne}})$, shown in Fig. 5, depends on the local density within the first solvent shell through the local Wigner-Seitz radius r_ℓ . The magnitude $|A|$ of the electron scattering length represents the minimum distance between the electron and a single perturber, while the local Wigner-Seitz radius represents the maximum distance between the electron and a single perturber in the Wigner-Seitz cell. Thus, $r_\ell - |A|$ gives the size of the “box” in which the quasi-free electron is confined during the electron/perturber interaction. Since $E_k(\rho_{\text{P}})$ is inversely proportional to this box size, the decrease in r_ℓ near the critical point (due to an increase in the local density) leads to a larger $E_k(\rho_{\text{P}})$. In the attractive rare gases Ar, Kr and Xe, the larger $|A|$ yields a smaller box size, even though r_ℓ for these gases is larger than that for Ne at the critical point [3–7]. The combination of these two effects on $P_-(\rho_{\text{P}})$ and $E_k(\rho_{\text{P}})$ leads $V_0(\rho_{\text{P}})$ to be strictly negative for Ar [3,4,7,9], Kr [5,7,9] and Xe [6,7], and strictly positive for Ne.

In conclusion, we have presented the first experimental results for $V_0(\rho_P)$ in a repulsive fluid from low density to the density of the triple point liquid, and we have interpreted these results within the local Wigner-Seitz model. We showed that the positive $V_0(\rho_{Ne})$ is due to a dominance of $E_k(\rho_{Ne})$ over the polarization energy; whereas, in the attractive rare gases [3–7], the larger polarization energies compensate for the zero-point kinetic energy, leading to a negative $V_0(\rho_P)$. When coupled to prior studies of attractive rare gases [3–7, 9, 10] and the attractive molecular gases CH_4 and C_2H_6 [8], the present work demonstrates that the local Wigner-Seitz model is widely applicable and yields significant insight into electron interactions in dense fluids.

Acknowledgements

The experimental measurements reported here were performed at the University of Wisconsin Synchrotron Radiation Center (NSF DMR-0537588). This work was supported by grants from the Petroleum Research Fund (45728-B6), from the Louisiana Board of Regents Support fund (LEQSF (1997-00)-RD-A-14), and from the Professional Staff Congress–City University of New York (62386-00 40). We thank Xiang Li, Feng Chen, Huixi Zhu and Cathy Le for their assistance in acquiring the data presented in Fig. 1.

References

- [1] S. C. Tucker, *Chem. Rev.* 99 (1999) 391, and references therein.
- [2] O. Kajimoto, *Chem. Rev.* 99 (1999) 355, and references therein.
- [3] C. M. Evans, G. L. Findley, *Chem. Phys. Lett.* 410 (2005) 242.

- [4] C. M. Evans, G. L. Findley, *J. Phys. B: At. Mol. Opt. Phys.* 38 (2005) L269.
- [5] Luxi Li, C. M. Evans, G. L. Findley, *J. Phys. Chem. A* 109 (2005) 10683.
- [6] Xianbo Shi, Luxi Li, C. M. Evans, G. L. Findley, *Chem. Phys. Lett.* 432 (2006) 62.
- [7] Xianbo Shi, Luxi Li, C. M. Evans, G. L. Findley, *Nucl. Inst. Meth. Phys. A* 582 (2007) 270.
- [8] Xianbo Shi, Luxi Li, G. L. Findley, C. M. Evans, *Chem. Phys. Lett.* 481 (2009) 183.
- [9] C. M. Evans, G. L. Findley, *Phys. Rev. A* 72 (2005) 022717.
- [10] Xianbo Shi, Luxi Li, Gina M. Moriarty, C. M. Evans, G. L. Findley, *Chem. Phys. Lett.* 454 (2008) 12.
- [11] A. K. Al-Omari, R. Reininger, *J. Chem. Phys.* 103 (1995) 506.
- [12] E. B. Gordon and B. M. Smirnov, *J. Exp. Theor. Phys.* 98 (2004) 924.
- [13] A. Henglein, *Can. J. Chem.* 55 (1977) 2112.
- [14] R. D. McCarty, R. B. Stewart, in S. Gratch (Eds.), *Advances in Thermophysical Properties at Extreme Temperatures and Pressures*, American Society of Mechanical Engineers, New York, 1965, p. 84.
- [15] J. Lekner, *Phys. Rev.* 158 (1967) 130.
- [16] E. W. Grundke, D. Henderson, R. D. Murphy, *Can. J. Phys.* 51 (1973) 1216.
- [17] F. M. Mourits, F. H. A. Rummens, *Can. J. Chem.* 55 (1977) 3007.
- [18] P. T. Sikora, *J. Phys. B: At. Mol. Opt. Phys.* 3 (1970) 1475.
- [19] W. Tauchert, H. Jungblut, W. F. Schmidt, *Can. J. Chem.* 55 (1977) 1860.

- [20] A. M. Koehler, R. Reininger, V. Saile, G. L. Findley, *Phys. Rev. A* 35 (1987) 79.
- [21] A. Garcia-Vela, J. Rubayo-Soneira, G. Delgado-Barrio, and P. Vilarreal, *J. Chem. Phys.* 104 (1996) 8405.

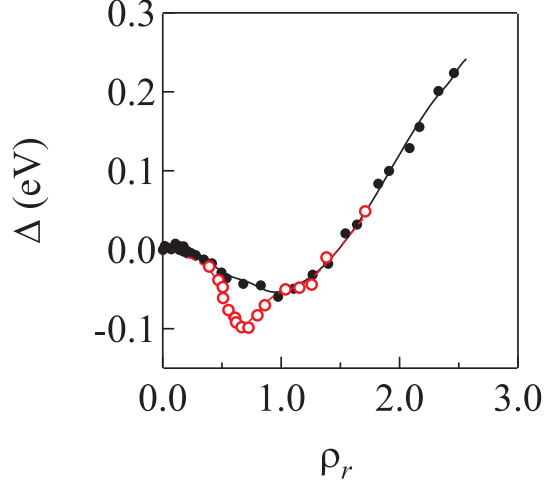


Fig. 1. [Color online] Ne induced shift $\Delta(\rho_{\text{Ne}})$ of the O_2 ionization energy plotted as a function of reduced Ne number density $\rho_r \equiv \rho_{\text{Ne}}/\rho_c$. (The critical density for Ne is $\rho_c = 14.4 \times 10^{21} \text{ cm}^{-3}$ [14].) (●) and (○) represent data obtained at noncritical temperatures and on an isotherm near the critical isotherm, respectively. The lines result from a fit to the local Wigner-Seitz model, as discussed below. The markers are approximately the size of the total experimental error.

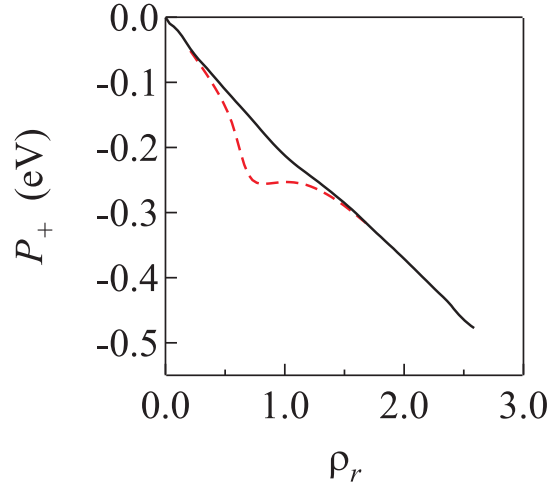


Fig. 2. [Color online] The ensemble-averaged O_2^+/Ne polarization energy $P_+(\rho_{\text{Ne}})$ calculated from eq. (4), plotted as a function of reduced Ne number density ρ_r . The solid and dashed lines represent calculations at noncritical temperatures and on an isotherm near the critical isotherm, respectively.

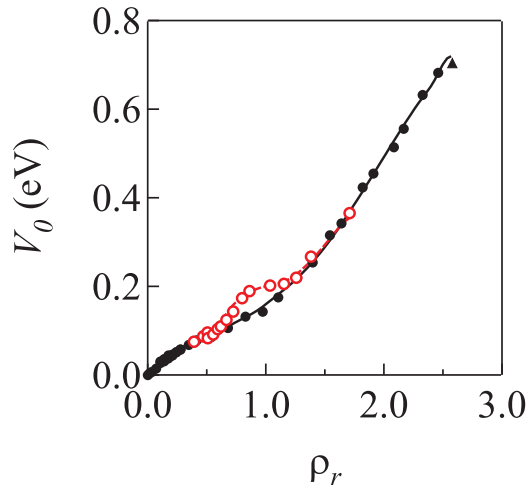


Fig. 3. [Color online] The minimum energy $V_0(\rho_{\text{Ne}})$ of the Ne conduction band plotted as a function of reduced Ne number density ρ_r . Solid markers represent data extracted from eq. (3) for noncritical isotherms, while the open markers are data obtained on an isotherm near the critical isotherm (i.e., $T_r = T/T_c \leq 1.02$). (\blacktriangle) represents a direct determination of $V_0(\rho_{\text{Ne}})$ for the triple point liquid [19]. The lines are local Wigner-Seitz calculations, details of which are given in the text.

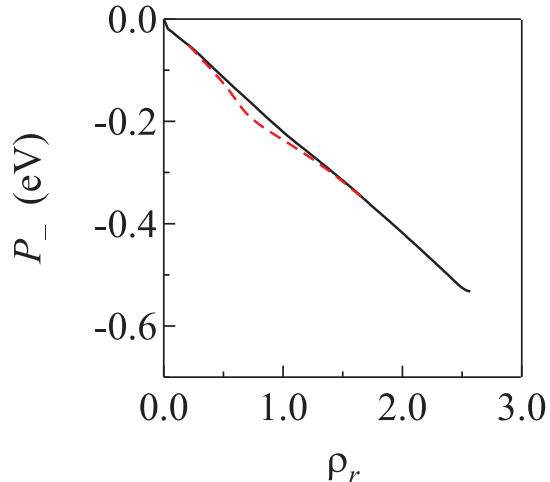


Fig. 4. [Color online] The ensemble-averaged electron/Ne polarization energy $P_-(\rho_{\text{Ne}})$ plotted as a function of reduced Ne number density ρ_r . The solid and dashed lines represent calculations at noncritical temperatures and on an isotherm near the critical isotherm, respectively. See text for discussion.

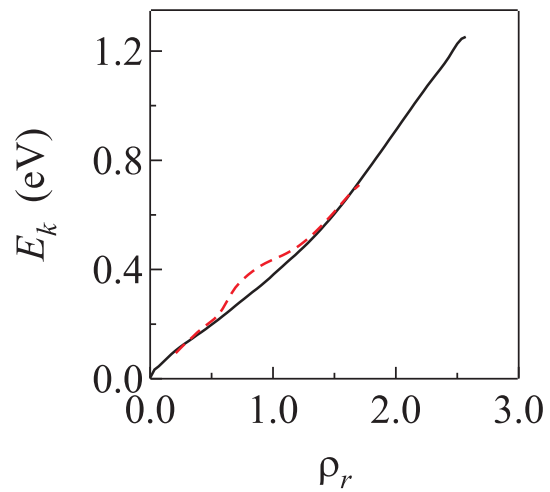


Fig. 5. [Color online] The zero-point kinetic energy $E_k(\rho_{\text{Ne}})$ of the quasi-free electron in Ne plotted as a function of reduced Ne number density ρ_r . The solid and dashed lines represent calculations at noncritical temperatures and on an isotherm near the critical isotherm, respectively. See text for discussion.